sustainability

MDPI

Article

Modeling and Predicting Land Use/Land Cover Change Using the Land Change Modeler in the Suluh River Basin, Northern Highlands of Ethiopia

Hailay Hagos Entahabu [1,2,*], Amare Sewnet Minale [1] and Emiru Birhane [3,4]

[1] Department of Geography and Environmental Studies, Bahir Dar University, Bahir Dar P.O. Box 79, Ethiopia; amare1974@gmail.com
[2] Department of Geography and Environmental Studies, Debre Tabor University, Debre Tabor P.O. Box 272, Ethiopia
[3] Department of Land Resources Management and Environmental Protection, Mekelle University, Mekelle P.O. Box 231, Ethiopia; emiru.birhane@mu.edu.et
[4] Institute of Climate and Society, Mekelle University, Mekelle P.O. Box 231, Ethiopia
* Correspondence: hailayhagos4@gmail.com

Abstract: Land use and land cover change are among the drivers of environmental change. The Suluh River Basin's land use and land cover are modeled in this study using a land change modeler. To accomplish the goals of this study, Landsat images and ancillary data sources were utilized. In eCognition Developer 9.2 software, nearest neighbor fuzzy classification was used to classify Landsat images. With the IDRISI Selva 17.3 software, change detection and modeling were carried out. Both qualitative and quantitative analyses of the data were conducted. The results showed that, despite a drop in forest land of 97.2%, grazing land of 89.8%, plantation land of 89.1%, shrub-bush land of 1.5%, and water bodies of 84.8% from 1990 to 2002, bare land increased by 10.6%, built-up land by 29.4%, and cultivated land by 65.4%. The model projects, bare, built-up, and cultivated land will increase at the cost of water bodies, grazing, forest, shrub-bush, and plantation land between the years 2028 and 2048. Rainfall, slope, height, distance to rivers, distance to highways, distance from towns, and population density were the main determinants of LULC change in the study area. Therefore, in order to promote sustainable development, safeguard the river basin, and lessen the severity of the changes, appropriate management and timely action must be taken by policymakers and decision makers.

Keywords: nearest neighbor fuzzy classification; change detection; land change modeler; Suluh River Basin

Citation: Entahabu, H.H.; Minale, A.S.; Birhane, E. Modeling and Predicting Land Use/Land Cover Change Using the Land Change Modeler in the Suluh River Basin, Northern Highlands of Ethiopia. *Sustainability* **2023**, *15*, 8202. https://doi.org/10.3390/su15108202

Academic Editors: Salvador García-Ayllón Veintimilla, Taixia Wu and Yongnian Gao

Received: 27 February 2023
Revised: 28 April 2023
Accepted: 3 May 2023
Published: 18 May 2023

1. Introduction

Changes in land use and land cover (hereafter LULC) are a major global environmental problem [1–3]. In recent decades, rapid changes have been occurring as a result of many anthropogenic influences [4–6], the consequences of which have altered the interaction between the earth's surfaces [7–11]. The study in [9] states that most of the changes are from vegetation cover to cultivated land. Differences have also been found in the magnitude and direction of LULC change worldwide. For instance, the study in [12] claims that the expansion of agriculture in Africa is a driving factor for LULC changes.

LULC change studies in Ethiopia show that most LULC changes are from natural forests to cultivated land [13–20] and are caused by anthropogenic factors [5,21–25]. Moreover, in a different part of Ethiopia, research was conducted on LULC modeling and predication by the authors in [26–29], who predicted that LULC will change from vegetation to cultivated land. In contrast, a few studies in a different part of Ethiopia indicated an improvement in vegetation cover [5,30,31] due to community afforestation and land

rehabilitation activity. So, an empirical investigation of the issues of LULC at the local catchment level is needed.

Modeling of LULC change has grown rapidly to demonstrate the function of the LULC system [32]. Several studies, such as [33–40], have affirmed that, compared to other LULC modeling methods, the Land Change Model (hereafter LCM), based on integrated multilayer perceptron (hereafter MLP) with Markov chain (hereafter MC), is a strong model for the analysis and prediction of LULC change and provides valid results.

In the *Suluh River Basin* (hereafter SRB), population growth and a lack of alternative livelihood strategies have led to environmental degradation [41–44]. Due to the lack of available land, farmers have no choice but to: (1) acquire more land by expanding into steep and marginal areas in order to make up for the low yields from their current holdings; (2) change the type of crops grown on their former cropland or convert it to eucalyptus plantations; and (3) allow constant farming, excessive grazing, and the use of agricultural inputs. The studies in [41–44] conducted an analysis on LULC change in the *Tekeze* River Basin with different Spatio-temporal coverage and methodologies. However, there was no mention of modeling LULC change using LCM in the SRB. In this study, we use LCM to model and forecast LULC change in the SRB. We anticipate that the findings of this study will assist stakeholders and policymakers in land management and land use planning.

2. Materials and Methods

2.1. The Study Area: Suluh River Basin

The SRB is found in the northeastern part of Tigray, northern Ethiopia. The geographic location of the SRB extends from 39°24′59.06″ E to 39°26′22.73″ E latitude and 13°38′18.27″ N to 14°13′53.29″ N longitude (Figure 1). The total area covered by the SRB is about 930 km^2 and its elevation varies from 1700 to 3298 m above sea level. The study watershed falls in four districts (Saesie *Tsaeda Emba*, *Hawuzen*, *Kiltie Awlealo*, and *Degua Tembien*) of the eastern and south-eastern zones of Tigray.

The SRB is categorized as having a semi-arid climate. The warmest months are May and June, and the coldest months are December and January. The total annual rainfall and average temperature between 1988 and 2018 were about 420.4 mm and 17.5 °C, respectively (Figure 2). The rainfall season is between June and early September, and the rain is distributed mono-modally. Regarding the hydro-logical conditions, the drainage pattern of the SRB is dendrite [44]. Regarding the geology of the basin, trap basalt accounts for 2.8%, granite and shale account for 1.8%, metamorphic rock accounts for 28.9%, limestone accounts for 13.9%, and sandstone accounts for 52.7% [44]. The major soil types of the SRB area are *haplic lixisols*, which cover 41.4%, *lithic leptosols*, which cover 22.7%, *Eutric leptosols*, which cover 17.8%, *Chromic Cambisols,* which cover 15.6%, and *Vertic Cambisols*, which cover 2.5%. Regarding the major soil textures of the study area, sandy clay loam accounts for 41.4%, sandy loam accounts for 40.5%, and clay accounts for 18.2% [44].

According to the Ethiopian population census of 2007, the population density of the SRB was 142 persons/km^2 [45]. The main crops are cultivated in the highlands (barley, wheat, maize, teff, and pulses) and lowlands (Sorghum). Cultivation is carried out using the traditional ox-drawn plow. This area suffers from a livestock (cattle, sheep, goats, donkeys, and chickens) feed crisis, resulting from crop residue and vegetation biomass reduction [41–43]. Most of the areas are highly cultivated, which leads to overgrazing and deforestation. Building stone terraces, micro dams, exclosures, and community woodlots, as well as enforcing rules and regulations for grazing lands and reducing burning activities, are some of the major methods of land management in the SRB [43,44,46].

2.2. Sources and Analyses of Data for LULC Change Detection and Prediction

Data pre-processing, data post-processing, and LULC change modeling were all carried out in accordance with the overall workflow shown in Figure 3. Free satellite photos from the National Aeronautics and Space Administration (Landsat-5 TM of 1990, Landsat-7

ETM+ of 2002, and Landsat-8 OLI-TIRS of 2018) were utilized for the LULC change analysis and modeling of the research region (Table 1).

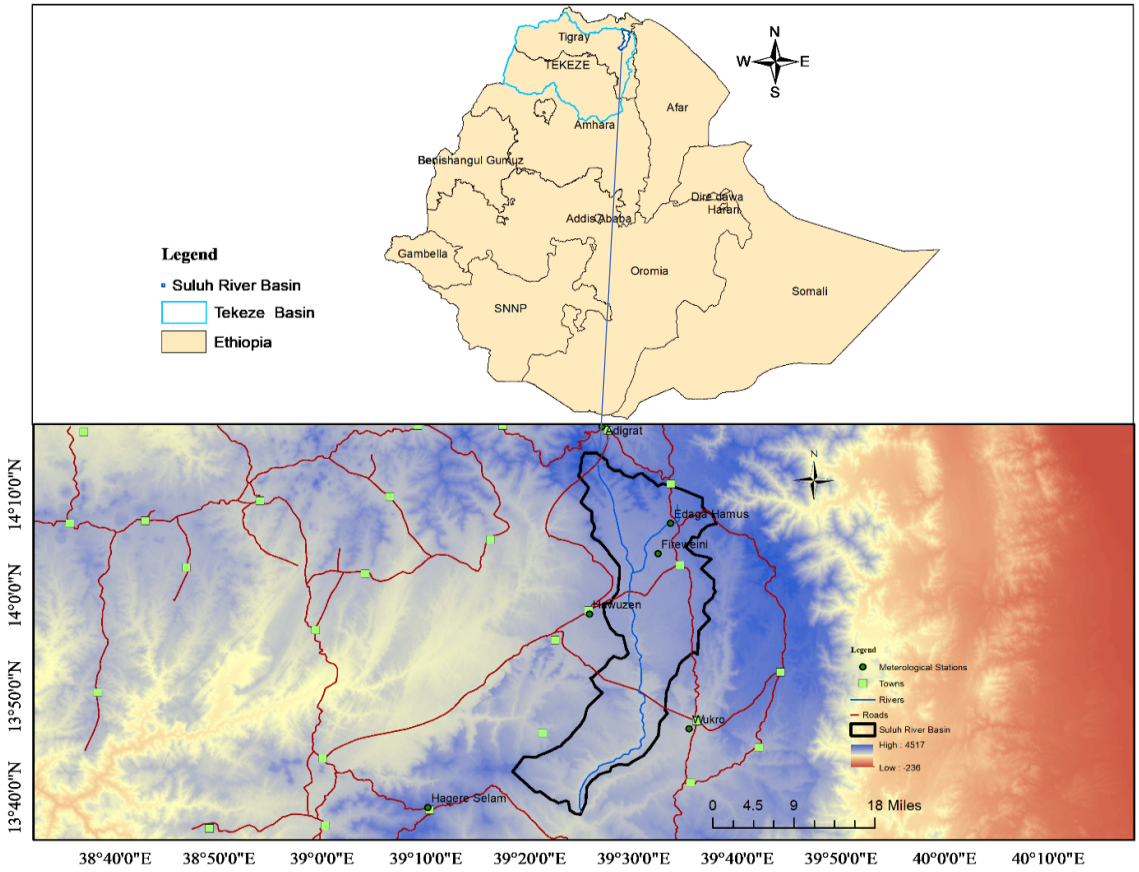

Figure 1. Location map of the study area, Suluh River Basin in Tigray, northern Ethiopia.

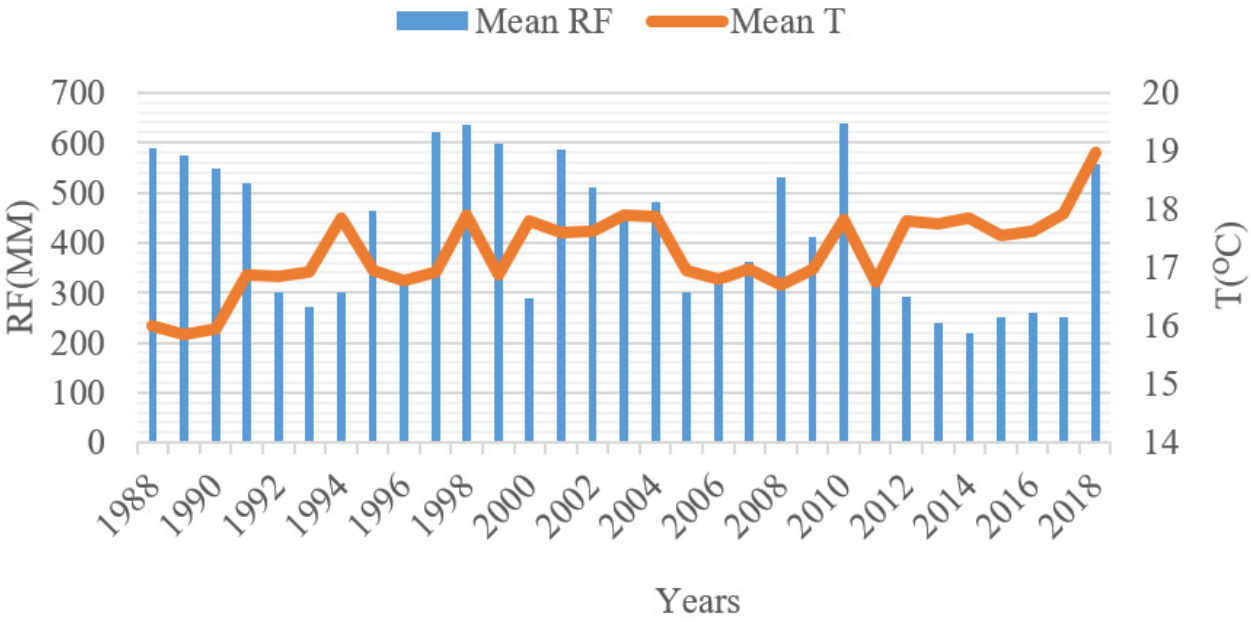

Figure 2. Mean annual rainfall (RF) and Mean Temperature (T) of the *Suluh River Basin* for the period 1988–2018 (sources station data).

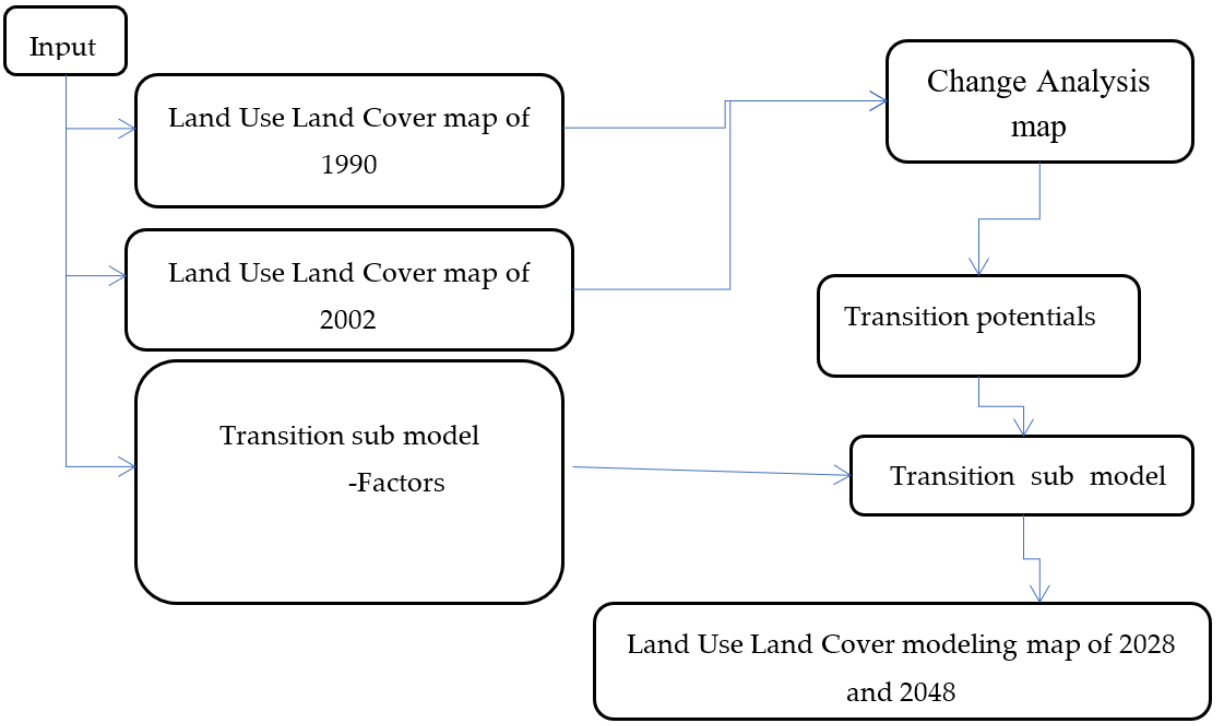

Figure 3. Methodology Flow Chart for Land Change Modeler.

Table 1. The characteristics of Landsat data.

Sensor	Path/Row	Acquisition Time	Spatial Resolution Resolution	Sensor
Landsat TM	169/50	1 January 1990	30 m	TM
Landsat ETM+	169/50	3 February 2002	15 m	ETM^{+}
Landsat OLI-TIRS	169/50	3 March 2018	15 m	OLI-TIRS
Aster DEM			30 m	
Ancillary data				
Topo map			1:50,000	
Field data			November 2017–January 2018	
Roads and towns				
District boundary				
Village boundary				

The Landsat-7 ETM+ 2002 and Landsat-8 OLI–TIRS 2018, 30 m pixel, were resampled to a 15 m pixel size. The Digital Elevation Model (30 m) based on Aster imagery and ancillary data (topographic maps, field thematic layers (roads and towns), and village and district boundaries) were also utilized during the analysis. These datasets were acquired from the National Aeronautics and Space Administration (NASA) through their EOS Data Gateway Database. All data were projected using the Universal Transverse Mercator projection system, zone 37° N, and datum of the World Geodetic System 84 (WGS84). Intensive pre- and post-processing of images was also carried out in ERDAS imagine 2015 software.

In *eCognition Developer* 9.2, we used the nearest neighbor fuzzy (Equation (1)) classification. It is used in *eCognition* automatically by generating multidimensional membership functions [47–54]. Based on Table 2, we created eight LULC groups (cultivated, bar, built up, grazing, plantation, shrub-bush, water body, and forest land).

Table 2. Land cover, Land use types and their descriptions.

LU/LC Classes	Descriptions
CL	Areas covered by crops in both irrigation and subsistence farming.
FL	Areas covered by forests mainly better canopy
GL	Areas covered by grasses including the closed and free grazing land
SBL	This category contains low woody plants that typically grow vertically and are less than three meters tall with many stems.
BL	Vacant spaces with little to no vegetation cover that may also have exposed soil or bedrock.
BUL	Areas for construction sites and towns
PL	Areas composed of Cactus, *Eucalyptus globules* and *Cupresus* spp.
WB	Includes lakes (both man-made and natural lakes), rivers, and reserves, among other things.

Note: Forest land (FL), cultivated land (CL), shrub-bush land (SBL), built up land (BU), grazing land (GL), bare land (BL), plantation land (PL) and water body (WB).

$$A = \{(X, \mu A(x)); x\epsilon \text{ X}\}, \text{where } \mu\text{A } \rightarrow [0, 1] \quad (1)$$

where A = fuzzy set X = a space of objects X = elements belonging to space X μ–membership function. In this work, the classification accuracy of the images was evaluated using the overall accuracy (Equation (2)) and Kappa coefficient (Equation (3)). The kappa coefficient data show good accuracy, with values of 0.886, 0.883, and 0.852 for the years 1990, 2000, and 2018, respectively (Table 3), since the values are above the typical overall classification accuracy level cutoff of 85% [34,55–58], with no class having a score below 70% [34].

$$\text{OA} = \frac{X}{Y} * 100 \quad (2)$$

where OA is overall accuracy, X is the number of correct values in diagonals of the matrix, and Y is the total number of values taken as a reference point.

$$K = N \sum_{i=1}^{r} xii - \sum_{i=1}^{r} (xi \times x + 1) / \; N2 - \sum_{i=1}^{r} xii - \sum_{i=1}^{r} (xi * x + 1) \quad (3)$$

where: r = is the number of rows in the matrix

Table 3. Summary of error matrixes for the classified images of 1990 and 2002.

LULC Classes	1990		2002	
	User Accuracy	Producer Accuracy	User Accuracy	Producer Accuracy
BL	56%	100%	65%	100%
BUL	88%	100%	89%	100%
CL	100%	55%	100%	56%
FL	100%	94%	100%	100%
GL	100%	94%	100%	100%
PL	86%	100%	88%	100%
SBL	78%	100%	79%	100%
WB	94%	100%	100%	100%
Overall Accuracy	87.12121212		89.79592	
Kappa Accuracy	0.852591473		0.883327	

Xii = is the number of observations in rows *i* and column *i* (along the major diagonal), *Xi*+ = the marginal total of row i (right of the matrix), *Xi* + 1 are the marginal totals of column *i* (bottom of the matrix), and *N* is the total number of observations. *K* = kappa coefficient.

LULC Modeling Using LCM

The LCM model predicts LULC changes from the thematic raster images with the same number of classes in the same sequential order [35–37,59–66]. The LCM is used to predict future LULC changes in the SRB for the next 30 years by following four steps.

The first is change analysis, hence the changes between two different periods (time 1 (1990) time 2 (2002)). LULC maps were calculated using the formula in [67] (Equation (4)):

$$C = \frac{\Delta f - \Delta i}{\Delta i} \times \frac{1}{T} \times 100 \quad (4)$$

where C = is the annual change rate of a given LULC type, Δf and Δi are the final and initial area coverage of LULC type during the specific period, and T = year difference between the initial and final period.

The gain and loss (Equation (5)) were also calculated using LCM in IDIRISI selva 17.3 software.

$$\begin{aligned} &[\mathrm{Ploss(i),j} = (\mathrm{Pj,i} - \mathrm{pi,j})/(\mathrm{pi} - \mathrm{pi}) * 100\ \mathrm{i\#j}] \\ &[\mathrm{Pgain(i),j} = (\mathrm{Pj,i} - \mathrm{pi,j})/(\mathrm{pi} - \mathrm{pi}) * 100\ \mathrm{i\#j}] \end{aligned} \quad (5)$$

where Ploss(i), j Is the percentage taken by j in LUCC in total 'conversion loss' of category row i Pgain(i), j Is the percentage taken by j in LULC change in total 'conversion gain' of category row i, pi,j and $p_{j,i.}$

Modeling transition potential and determining driving forces is the second phase [68,69]. The characteristics found were to be biophysical (rainfall, slope, and elevation), socioeconomic (distance to rivers, distance to highways, distance to towns), and demographic (population density). Cramer's V coefficient was utilized for model variable testing, selection, and transition. The transition sub-model was then updated to include all the variables. MLP neural networks were utilized to run the model and organize the transition sub-model. The training set and the testing set each received a random group of transition pixels that would appear between 1990 and 2002. The variables were derived via geographical and geo-statistical elaborations of a geographic information system and were formalized as follows (Equation (6))

$$X = X1, X2, \ldots, Xn \quad (6)$$

Every variable associated with a neuron in the input layer was normalized using (Equation (7)):

$$X = (x_i - min)/(max - min)\ \mathrm{X} = (\mathrm{X}i - min)/(\mathrm{maxmin}) \quad (7)$$

In the hidden layer, the signal that is received by neuron j in the hidden layer for pixel k was calculated as follows (Equation (8)):

$$net\mathrm{j}\ (k,t) = \sum_i \mathrm{Wi,j\ Xi(k)} \quad (8)$$

where *net*j(*k*,*t*) is the signal that is received by neuron j, and *w*i,j is the weight between the input layer *I* and the hidden layer *j*. The output layer has two neurons that correspond to two possible significant states (1 = transition, 2 = permanence of the pixel); neuron *l* generates a value that indicates the transition probability. Transition probabilities can be calculated using a sigmoidal function using Equation (9). (A sigmoidal function is used to represent the non-linearity of each node):

$$\mathrm{P(k.1)} = \sum_i \mathrm{Wj,i} \frac{1}{1 + x^{netj(k,t)}} \quad (9)$$

The third and fourth steps are change prediction and future scenarios. Change prediction is executed based on MC, using the historical rate of change and the transition potential maps [70]. MC analyses were run for this study to determine the amount of change using two LULC maps (1990 and 2002) along with the date specified (2018, 2028 and 2048). The steps determine how much land was expected to transition from the later date (2002) to the prediction date (2028 and 2048). An MC (Equation (10)) comprises s, a vector of the distribution of LULC classes at time t, and A(ϒ), a matrix of transition probabilities from land use u to land use u′ in a given time interval (ϒ)

$$St + \Upsilon = A(\Upsilon)St \quad (10)$$

Validating the model is the fifth stage. A comparison of the simulated and actual LULC maps from 2018 was made in this study as part of the validation process. While quantitative data were collected and analyzed using descriptive statistics, the qualitative material collected through direct observation, focus group discussions, and interviews was analyzed and interpreted using qualitative approaches (such as a percentage).

3. Results

3.1. LULC Change Analysis from 1990 to 2002

According to Table 4, the LULC change trend showed that from 1990 to 2002, the LULC in FL, GL, PL, SBL, and WB decreased by 97.2%, 89.8%, 89.1%, 1.5%, and 84.8%, respectively. However, the BL, BUL, and CL all increased by 10.6%, 29.4%, and 65.4%, respectively. Elder priest interviewees agreed that there was more vegetation cover in church woodlands in 1990 than there was in 2002. The panelists from the focus group agreed that there had been significant land fragmentations as a result of repeated land redistribution. The district office of agriculture and rural development was contacted for an interview; they stated that LULC change has been hampered due to the population density in the river basin.

Table 4. LULC Change trends in from 1990 to 2048.

LULC Classes	LULC Area (km^2)					Trends of Change (%)		
	1990	2002	2018	2028	2048	1990–2002	2018–2028	2018–2048
BL	82.5	91.2	90.6	92	94.2	11	0.6	2.2
BUL	12.7	16.4	29.9	33	38.7	29	1	5.7
CL	351	580.5	551	586	592	65	0.6	6.1
FL	24.4	0.7	10.3	8	6	–97	−2	−2
GL	186	18.9	95.6	73	65.4	−90	−2	−7.7
PL	46.7	5.1	67.2	71	76	−89	0.6	5
SBL	219	216.1	84.1	66	57	−1.5	−2	−9
WB	7.6	1.2	1.54	1.02	0.68	−85	−3	−0.3

The gains and losses of key LULC alterations are depicted in Figure 4A. They include (1) an expansion of CL, (2) an increase in BL, and (3) an increase in BUL, as well as a drop in SBL, GL, PL, and WB. During 1990–2002, gain and loss in CL were 359.94 km^2 and 33.03 km^2, with a net gain of 326.91 km^2. SBL lost 243.67 km^2 and gained 5.33 km^2, with a net loss of −238.34 km^2. PL lost 1.96 km^2 and gained 52 km^2 with a net loss of 50.04 km^2.

3.2. Transition Potential Modeling, Determining Driving Variables, LULC Transition Analysis and Validations

Population density (0.345), slope (0.25), elevation (0.18), rainfall (0.22), and the distance from the river (0.31), towns (0.27), and roads (0.17) were all found to have a substantial influence on LULC change in the research area using Cramer's V values as given in Table 5. Kappa variations that compared the projected LULC map with the actual LULC map of the year 2018 resulted in a Kappa value = 0.97, Kno = 0.97, Kappa location = 0.99, and k standard = 0.96. As indicated in Figure 5 and Table 6, both kappa results confirm that the

model is reliable for the SRB. Using a multilayer perceptron with an accuracy of over 70%, transitions were represented in a single transition sub-model once the predictor variables were chosen. The research area's water body, forest, grazing, and shrub-bush land were found to have significantly decreased as a result of the significant increase in CL, BL, and BU, according to the transition probability matrix, which compares probabilities between two different times (Tables 7–9).

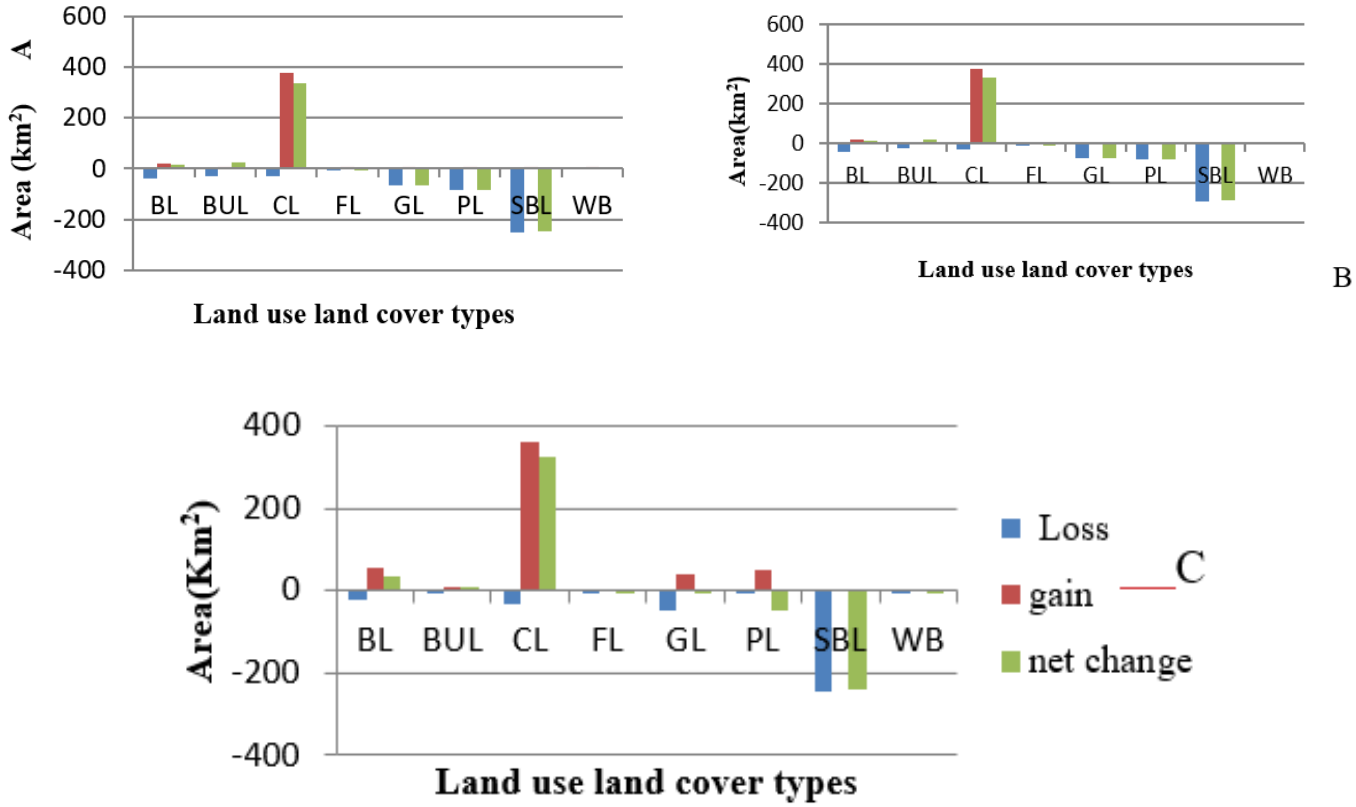

Figure 4. The gains and losses of LULC types of SRB in 1990 (**A**), 2002 (**B**), and 2018 (**C**).

Table 5. Cramer's V values of explanatory variables.

Explanatory Variables	Cramer's V
Rainfall	0.2162
slope	0.2526
Elevation	0.1787
distance to rivers	0.3107
distance to roads	0.1687
distance towns	0.2665
population density	0.3448

3.3. Future Scenario/Simulation

Based on real LULC maps, the model predicted LULC change for the years 2028 and 2048 (Figure 6). The Markov model also provides the transition probability matrix for the years 2028 and 2048 (Table 4). From the year 2018 to 2028, the trend of LULC change in the study area will show a decrease in FL, GL, SBL, and WB by 2%, 2%, 0.6%,3%, respectively (Table 4 and Figure 7), whereas BL, BUL, CL and PL areas will be increased by 0.6%, 1%, 0.6%,0.6%, respectively. As indicated in Figure 4B, during 2018–2028, gain and loss in CL were 374.31 km^2 and 31.38 km^2, with a net gain of 335.13 km^2. SBL lost 289.29 km^2 and gained 5.87 km^2, with a net loss of −283.22 km^2. PL lost 80.09 km^2 and gained 3.02 km^2, with a net loss of 77.07 km^2.

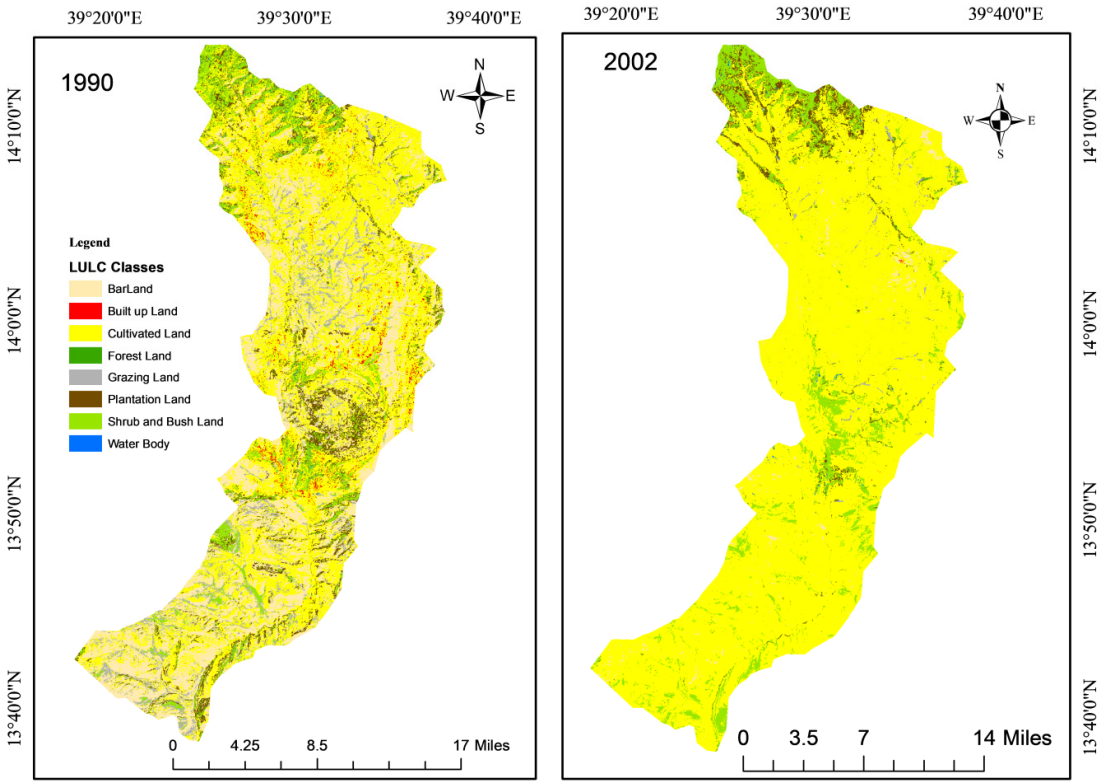

Figure 5. Land use/cover map of study area for 1990 and 2002.

Table 6. Area statistics of actual and predicted land use/land cover map of 2018.

LULCT	Actual	Predicted
BL	92	86
BUL	33	38
CL	586	602
FL	8	4.28
GL	73	62
PL	71	75
SBL	66	62
WB	1.02	0.74
	930.02	930.02

Table 7. Transition probability matrix of land use/land cover classes for the year 2018.

LULCT	BL	BUL	CL	FL	GL	PL	SBL	WB
BL	0.0096	0	0.9485	0.0007	0.004	0.0047	0.0325	0
BUL	0.0034	0.0015	0.9894	0.0001	0	0.0024	0.0031	0.0001
CL	0.0045	0.0003	0.9347	0.0002	0.0011	0.0222	0.0366	0.0004
FL	0	0	0.1788	0.1026	0.0244	0.1212	0.5725	0.0005
GL	0.0002	0	0.8903	0.002	0.0391	0.0047	0.0635	0.0002
PL	0.0001	0.0001	0.5642	0.0048	0.0042	0.0952	0.3301	0.0014
SBL	0.0001	0.0003	0.4061	0.0039	0.0028	0.1113	0.4664	0.0092
WB	0.0014	0	0.2143	0.0014	0	0.0844	0.6878	0.0109

Table 8. Transition probability matrix of land use/land covers classes for the year 2028.

LULCT	BL	BUL	CL	FL	GL	PL	SBL	WB
BL	0.0106	0.0003	0.9053	0.0005	0.0013	0.0256	0.0557	0.0007
BUL	0.0109	0.0003	0.9177	0.0004	0.0012	0.0235	0.0456	0.0005
CL	0.0105	0.0002	0.8979	0.0005	0.0013	0.0269	0.0618	0.0008
FL	0.0033	0.0002	0.5752	0.0056	0.0034	0.0820	0.3249	0.0054
GL	0.0102	0.0002	0.8893	0.0007	0.0015	0.0283	0.0688	0.0010
PL	0.0071	0.0002	0.7471	0.0020	0.0020	0.0530	0.1856	0.0031
SBL	0.0056	0.0002	0.6802	0.0025	0.0022	0.0646	0.0646	0.0041
WB	0.0037	0.0002	0.5946	0.0032	0.0025	0.0794	0.3111	0.0053

Table 9. Transition probability matrix of land use/land covers classes for the year 2028.

LULCT	BL	BUL	CL	FL	GL	PL	SBL	WB
BL	0.29	0.68	0	0.02	0	0	0	0
BUL	0.19	0.76	0	0.02	0.001	0.0012	0	0
CL	0.28	0.67	0	0.04	0.006	0.005	0.0001	0
FL	0.07	0.6	0.03	0.12	0.12	0.06	0.007	0
GL	0.15	0.5	0.06	0.1	0.14	0.02	0.001	0
PL	0.06	0.54	0.01	0.27	0.1	0.0098	0.0012	0
SBL	0.08	0.52	0.01	0.2	0.15	0.0199	0.0011	0
WB	0.12	0.55	0.01	0.18	0.11	0.019	0.009	0

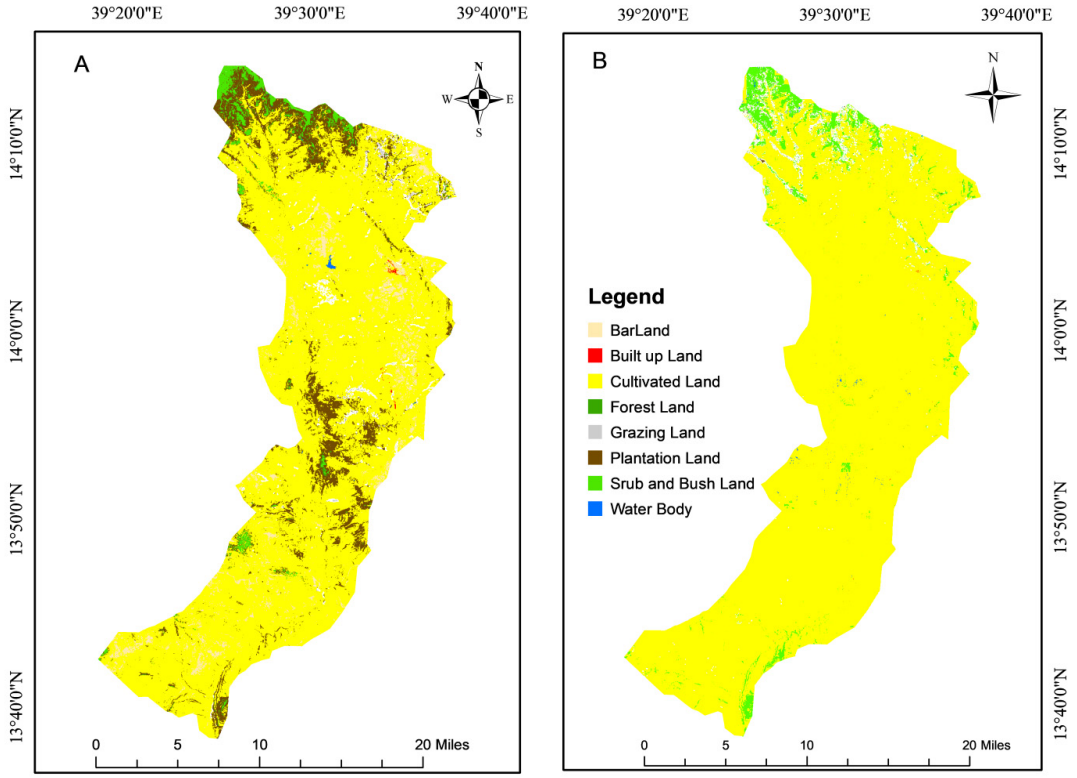

Figure 6. The simulated (**A**) and the actual (**B**) land use/land cover of the *SRB* in 2018.

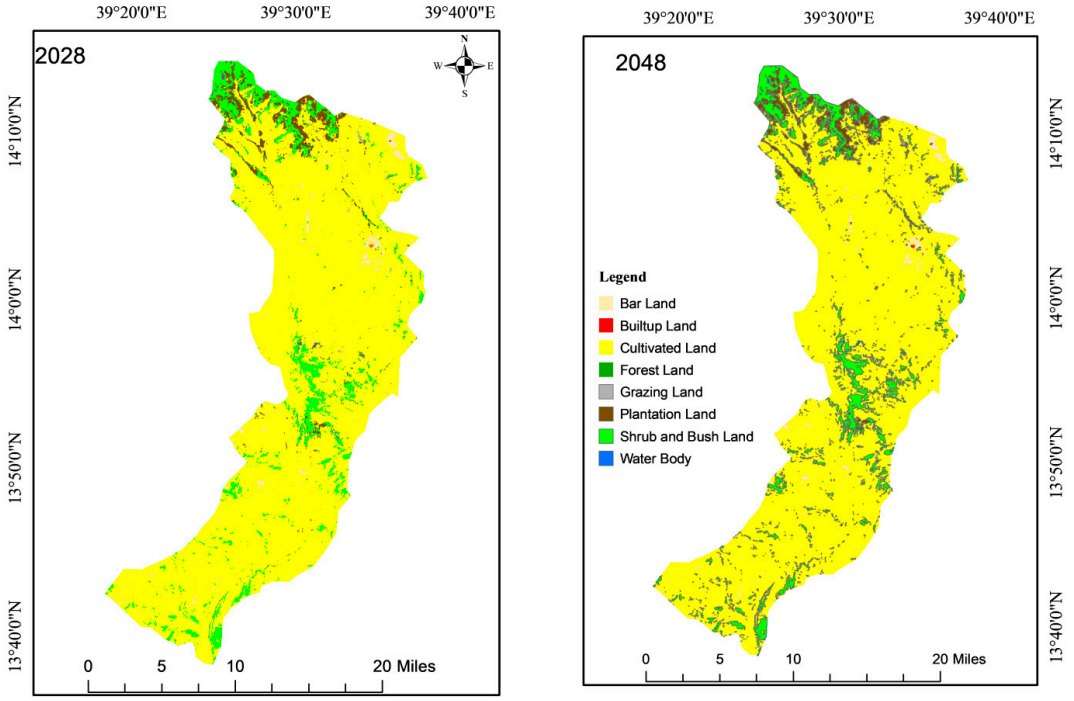

Figure 7. The 2028 and 2048 land use/land cover of the SRB.

Table 4 shows that the LULC trends for bar land, built-up land, plantation land, and cultivated land will increase from 2018 to 2048 by 2.2%, 5.7%, 5%, and 5.7%, respectively. On the other hand, between 2018 and 2048, the FL, GL, SBL, and WB areas will grow by 2%, 7.7%, 9%, and 0.3%, respectively. According to Figure 4C, between 2018 and 2048, CL will acquire and lose 378.14 km^2 and 31.7 km^2, respectively, with a net gain of 338.56 km^2. With a gain of 5.03 km^2 and a loss of 249.84 km^2, SBL will exhibit a net loss of −244.6 km^2. PL lost 82.5 km^2 overall, gaining 3.23 km^2, and losing 85.73 km^2. However, there was a net gain of 16.2 km^2 in built-up land.

4. Discussion

The study's results showed an increase in BUL, CL, and BL from 1990 to 2002, which will persist until 2048. The sharp decline in WB, FL, GL, PL, and SBL that was seen between 1990 and 2002 will last until 2048.The study's findings are consistent with those of earlier research projects carried out in Ethiopia by the authors in [71] in the Birr and Upper Didesa watersheds of the Blue Nile basin, as well as those described in [72] for the Dera area in northwest Ethiopia. The findings of the study show that BUL, CL, and BL increase, which is consistent with other research findings in Africa [73] and Ethiopia [14,29], as well as studies in some parts of Europe, such as in Slovakia [74], Portugal Poland, and Czechia. Contrasting findings were indicated by [5,30,31,75], which confirmed increasing vegetation cover due to integrated watershed management in the *Tekeze* basin [76–78].

Different kinds of LULC change drivers have been discovered in various regions of Ethiopia. For instance, the studies in [5,16] indicated human drivers, the one in [14] identified population growth; the research in [78] showed land degradation, poverty, and food insecurity; the authors in [29] identified population, slope, livestock, and distances from various infrastructures; and the study in [29] also identified population pressure, income growth, and declining productivity. Ref. [79] found that slope, distance from the stream, distance from urban areas, and distance from roads also play an important role in land use change, as each provides residents with convent access to resources. In our study, the factors that affected LULC in the SRB included rainfall, slope, elevation, distance to rivers, distance to highways, distance to towns, and population density. Consideration

of the drivers of LULC changes at the watershed level is of paramount importance for sustainably managing the environment in that watershed.

This study used LCM in the SRB to accomplish LULC modeling. This model is effective because it can simulate various types of land cover with adequate calibration and dynamic projection skills [80,81]. Various studies have also demonstrated that LCM is effective at predicting LULC change [82–87]. Therefore, the findings would be useful as inputs for planners and other stakeholders regarding LULC trends in the study area.

5. Conclusions and Recommendations

The current study was carried out to model and predict land use/land cover changes from 1990 to 2048 using LCM in the SRB, Ethiopia. Bar land, built-up land, and cultivated land will increase at the expense of water bodies, forests, shrub-bush, and plantation land in the years 2028 and 2048. Rainfall, slope, elevation, distance to rivers, distance to roads, distance towns, and population density were identified as the prominent LULC change drivers in the study area. This will increase the vulnerability of the watershed to soil erosion and soil macrofauna loss in the studied river basin in particular and the *Tekeze* basin in general. Therefore, suitable and timely management measures must be taken by policymakers and decision-makers to enable sustainable development and protect the river basin to reduce the severity of the changes.

Author Contributions: H.H.E. participated in proposing the study, managed all data collection, conducted all data analyses performed statistical analyses and interpretation results, and drafted the manuscript. A.S.M. as supervisors participated in guiding and reviewing the manuscript. E.B. was supervisor and participated in designing the field study and reviewed the manuscript. All authors have read and agreed to the published version of the manuscript.

Funding: This research was funded by Debre Tabor University, Ethiopia and Bahir Dar University, Ethiopia.

Institutional Review Board Statement: Not applicable.

Informed Consent Statement: Not applicable.

Data Availability Statement: Not applicable.

Acknowledgments: The authors would like to thank Bahir Dar University and Debre Tabor University in Ethiopia for their financial support. The authors greatly acknowledge farmers and the agricultural development agents of the Watershed for their interest to focus group discussions and for providing necessary information.

Conflicts of Interest: The authors declare no conflict of interest.

References

1. Shafizadeh Moghadam, H.; Helbich, M. Spatiotemporal urbanization processes in the megacity of Mumbai, India: A Markov chains-cellular automata urban growth model. *Appl. Geogr.* **2013**, *40*, 140–149. [CrossRef]
2. Meyfroidt, P.; Lambin, E.F.; Erb, K.-H.; Hertel, T.W. Globalization of land use: Distant drivers of land change and geographic displacement of land use. *Curr. Opin. Environ. Sustain.* **2013**, *5*, 438–444. [CrossRef]
3. Wnęk, A.; Kudas, D.; Stych, P. National Level Land-Use Changes in Functional Urban Areas in Poland, Slovakia, and Czechia. *Land* **2021**, *10*, 39. [CrossRef]
4. Houghton, R.A. The Worldwide Extent of Land-Use Change. *Bioscience* **1994**, *44*, 305–313. [CrossRef]
5. Bewket, W. Land covers dynamics since the 1950s in Chemoga watershed, Blue Nile basin, Ethiopia. *Mt. Res. Dev.* **2002**, *22*, 263–269. [CrossRef]
6. Bewket, W.; Abebe, S. Land-use and land-cover change and its environmental implications in a tropical highland watershed, Ethiopia. *Int. J. Environ. Stud.* **2013**, *70*, 126–139. [CrossRef]
7. Fu, X.; Wang, X.; Yang, Y.J. Deriving suitability factors for CA-Markov land use simulation model based on local historical data. *J. Environ. Manag.* **2018**, *206*, 10–19. [CrossRef] [PubMed]
8. Lambin, E.F.; Geist, H.J.; Lepers, E.; Meyer, W.B.; Turner, I.B.L.; Meyfroidt, P.; Alix-Garcia, J.; Wolff, H.; Bentley, J.W.; Innes, R.; et al. Dynamics of Land-Use and Land-Cover Change in Tropical Regions. *Annu. Rev. Environ. Resour.* **2003**, *28*, 205–241. [CrossRef]

9. Kabat, P.; Claussen, M.; Dirmeyer, P.A.; Gash, J.H.; de Guenni, L.B.; Meybeck, M.; Hutjes, R.W.; Pielke, R.A., Sr.; Vorosmarty, C.J.; Lütkemeier, S. (Eds.) *Vegetation, Water, Humans and the Climate: A New Perspective on an Internactive System*; Springer Science & Business Media: Berlin/Heidelberg, Germany, 2004.
10. Mahmood, R.; Pielke, R.A.; Hubbard, K.G.; Niyogi, D.; Bonan, G.; Lawrence, P.; McNider, R.; McAlpine, C.; Etter, A.; Gameda, S.; et al. Impacts of land use/land cover change on climate and future research priorities. *Bull. Am. Meteorol. Soc.* **2010**, *91*, 37–46. [CrossRef]
11. Prasad, P.R.C.; Rajan, K.S.; Dutt, C.B.S.; Roy, P.S. A conceptual framework to analyse the land-use/land-cover changes and its impact on phytodiversity: A case study of North Andaman Islands, India. *Biodivers. Conserv.* **2010**, *19*, 3073–3087. [CrossRef]
12. Wood, E.; Tappan, G.; Hadj, A. Understanding the drivers of agricultural land use change in south-central Senegal. *J. Arid. Environ.* **2004**, *59*, 565–582. [CrossRef]
13. Rientjes, T.H.M.; Haile, A.T.; Kebede, E.; Mannaerts, C.M.M.; Habib, E.; Steenhuis, T.S. Changes in land cover, rainfall and stream flow in Upper Gilgel Abbay catchment, Blue Nile basin—Ethiopia. *Hydrol. Earth Syst. Sci.* **2011**, *15*, 1979–1989. [CrossRef]
14. Tekle, K.; Hedlund, L. Land Cover Changes Between 1958 and 1986 in Kalu District, Southern Wello, Ethiopia. *Mt. Res. Dev.* **2000**, *20*, 42–51. [CrossRef]
15. Tsegaye, D.; Moe, S.R.; Vedeld, P.; Aynekulu, E. Land-use/cover dynamics in Northern Afar rangelands, Ethiopia. *Agric. Ecosyst. Environ.* **2010**, *139*, 174–180. [CrossRef]
16. Zeleke, G.; Hurni, H. Implications of Land Use and Land Cover Dynamics for Mountain Resource Degradation in the Northwestern Ethiopian Highlands. *Mt. Res. Dev.* **2001**, *21*, 184–191. [CrossRef]
17. Tegene, B. Land-Cover/Land-Use Changes in the Derekolli Catchment of the South Welo Zone of Amhara Region, Ethiopia. *East. Afr. Soc. Sci. Res. Rev.* **2002**, *18*, 1–20. [CrossRef]
18. Dessie, G.; Kleman, J. Pattern and Magnitude of Deforestation in the South Central Rift Valley Region of Ethiopia. *Mt. Res. Dev.* **2007**, *27*, 162–168. [CrossRef]
19. Gidey, E.; Dikinya, O.; Sebego, R.; Segosebe, E.; Zenebe, A. Modeling the Spatio-temporal dynamics and evolution of land use and land cover (1984–2015) using remote sensing and GIS in Raya, Northern Ethiopia. *Model. Earth Syst. Environ.* **2017**, *3*, 1285–1301.
20. Minale, A.S.; Gelaye, S. Vegetation vulnerability analysis by using GIS and remote sensing techniques: A case study of Sensawuha Watershed, Ethiopia. *Geojournal* **2019**, *86*, 475–488. [CrossRef]
21. Gebreslassie, H. Land use-land cover dynamics of Huluka watershed, Central Rift Valley, Ethiopia. *Int. Soil Water Conserv. Res.* **2014**, *2*, 25–33. [CrossRef]
22. Hamza, I.; Iyela, A. Land Use Pattern, Climate Change, and Its Implication for Food Security in Ethiopia: A Review. *Ethiop. J. Environ. Stud. Manag.* **2012**, *5*, 26–31. [CrossRef]
23. Chiemela, S.N.; Noulekoun, F.; Zenebe, A.; Abadi, N.; Birhane, E. Transformation of degraded farmlands to agroforestry in Zongi Village, Ethiopia. *Agrofor. Syst.* **2017**, *92*, 1317–1328. [CrossRef]
24. Hailemariam, S.N.; Soromessa, T.; Teketay, D. Land Use and Land Cover Change in the Bale Mountain Eco-Region of Ethiopia during 1985 to 2015. *Land* **2016**, *5*, 41. [CrossRef]
25. Sewnet, A. Land Use/Cover Change at Infraz Watershed, Northwestren Ethiopia. *J. Landsc. Ecol.* **2015**, *8*, 69–83. [CrossRef]
26. Demessie, E.T. *Soil Hydrological Impacts and Climatic Controls of Land Use and Land Cover Changes in the Upper Blue Nile (Abay) Basin*; CRC Press: Boca Raton, FL, USA, 2015.
27. Yalew, S.G.; Mul, M.L.; Van Griensven, A.; Teferi, E.; Priess, J.; Schweitzer, C.; Van Der Zaag, P. Land-Use Change Modelling in the Upper Blue Nile Basin. *Environments* **2016**, *3*, 21. [CrossRef]
28. Han, R. Land Use and Land Cover Mapping Using Fuzzy Logic. In *Ecosystem Assessment and Fuzzy Systems Management*; Springer: Cham, Switzerland, 2014; pp. 129–146.
29. Gashaw, T.; Tulu, T.; Argaw, M. Erosion risk assessment for prioritization of conservation measures in Geleda watershed, Blue Nile basin, Ethiopia. *Environ. Syst. Res.* **2017**, *6*, 1. [CrossRef]
30. Bantider, A.; Hurni, H.; Zeleke, G. Responses of rural households to the impacts of population and land-use changes along the Eastern Escarpment of Wello, Ethiopia. *Nor. Geogr. Tidsskr.-Nor. J. Geogr.* **2011**, *65*, 42–53. [CrossRef]
31. Munro, R.N.; Deckers, J.; Haile, M.; Grove, A.; Poesen, J.; Nyssen, J. Soil landscapes, land cover change and erosion features of the Central Plateau region of Tigrai, Ethiopia: Photo-monitoring with an interval of 30 years. *Catena* **2008**, *75*, 55–64. [CrossRef]
32. Nourqolipour, R.; Shariff, A.R.B.M.; Balasundram, S.K.; Ahmad, N.B.; Sood, A.M.; Buyong, T.; Amiri, F. A GIS-based model to analyze the spatial and temporal development of oil palm land use in Kuala Langat district, Malaysia. *Environ. Earth Sci.* **2014**, *73*, 1687–1700. [CrossRef]
33. Wang, J.; Maduako, I.N. Spatio-temporal urban growth dynamics of Lagos Metropolitan Region of Nigeria based on Hybrid methods for LULC modeling and prediction. *Eur. J. Remote Sens.* **2018**, *51*, 251–265. [CrossRef]
34. Kumar, K.S.; Bhaskar, P.U.; Padmakumari, K. Application of land change modeler for prediction of future land use land cover: A case study of Vijayawada City. *Int. J. Adv. Technol. Eng. Sci.* **2015**, *3*, 773–783.
35. Megahed, Y.; Cabral, P.; Silva, J.; Caetano, M. Land Cover Mapping Analysis and Urban Growth Modelling Using Remote Sensing Techniques in Greater Cairo Region—Egypt. *ISPRS Int. J. Geo-Inf.* **2015**, *4*, 1750–1769. [CrossRef]
36. Mas, J.-F.; Pérez-Vega, A.; Clarke, K.C. Assessing simulated land use/cover maps using similarity and fragmentation indices. *Ecol. Complex.* **2012**, *11*, 38–45. [CrossRef]

37. Mishra, V.N.; Rai, P.; Mohan, K. Prediction of land use changes based on land change modeler (LCM) using remote sensing: A case study of Muzaffarpur (Bihar), India. *J. Geogr. Inst. Jovan Cvijic SASA* **2014**, *64*, 111–127. [CrossRef]
38. Hasan, S.; Shi, W.; Zhu, X.; Abbas, S.; Khan, H.U.A. Future Simulation of Land Use Changes in Rapidly Urbanizing South China Based on Land Change Modeler and Remote Sensing Data. *Sustainability* **2020**, *12*, 4350. [CrossRef]
39. Kamusoko, C.; Aniya, M.; Adi, B.; Manjoro, M. Rural sustainability under threat in Zimbabwe—Simulationof future land use/cover changes in the Bindura district based on the Markov-cellularautomatamodel. *Appl. Geogr.* **2009**, *29*, 435–447. [CrossRef]
40. Ozturk, D. Urban Growth Simulation of Atakum (Samsun, Turkey) Using Cellular Automata-Markov Chain and Multi-Layer Perceptron-Markov Chain Models. *Remote Sens.* **2015**, *7*, 5918–5950. [CrossRef]
41. Alemayehu, F.; Taha, N.; Nyssen, J.; Girma, A.; Zenebe, A.; Behailu, M.; Deckers, S.; Poesen, J. The impacts of watershed management on land use and land cover dynamics in Eastern Tigray (Ethiopia). *Resour. Conserv. Recycl.* **2009**, *53*, 192–198. [CrossRef]
42. Aredehey, G.; Mezgebu, A.; Girma, A. Land-use land-cover classification analysis of Giba catchment using hyper temporal MODIS NDVI satellite images. *Int. J. Remote Sens.* **2018**, *39*, 810–821. [CrossRef]
43. Hishe, S.; Bewket, W.; Nyssen, J.; Lyimo, J. Analysing past land use land cover change and CA-Markov-based future modelling in the Middle Suluh Valley, Northern Ethiopia. *Geocarto Int.* **2020**, *35*, 225–255. [CrossRef]
44. Zenebe, A.; Vanmaercke, M.; Guyassa, E.; Verstraeten, G.; Poesen, J.; Nyssen, J. The Giba, Tanqwa and Tsaliet Rivers in the Headwaters of the Tekezze Basin. In *Geo-Trekking in Ethiopia's Tropical Mountains*; Springer: Cham, Switzerland, 2019; pp. 215–230. [CrossRef]
45. Population Census Commission; Summary and Statistical Report of the 2007 Population and Housing Census Results. Available online: http//www.csa.gov.et (accessed on 26 March 2022).
46. Sembroni, A.; Molin, P.; Dramis, F.; Abebe, B. Geology of the Tekeze River basin (Northern Ethiopia). *J. Maps* **2017**, *13*, 621–631. [CrossRef]
47. Foody, G.M. Status of land cover classification accuracy assessment. *Remote Sens. Environ.* **2002**, *80*, 185–201. [CrossRef]
48. Groenemans, R.; Van Ranst, E.; Kerre, E. Fuzzy relational calculus in land evaluation. *Geoderma* **1997**, *77*, 283–298. [CrossRef]
49. Kalantar, B.; Mansor, S.B.; Sameen, M.I.; Pradhan, B.; Shafri, H.Z.M. Drone-based land-cover mapping using a fuzzy unordered rule induction algorithm integrated into object-based image analysis. *Int. J. Remote Sens.* **2017**, *38*, 2535–2556. [CrossRef]
50. Kumar, P.; Ravindranath, S.; Raj, K.G. Object oriented classification and feature extraction for parts of east delhi using hybrid approach. *ISPRS-Int. Arch. Photogramm. Remote Sens. Spat. Inf. Sci.* **2018**, *XLII-5*, 749–754. [CrossRef]
51. Salman, A.A.; Ali, A.E.; Mattar, H.E. Mapping land-use/land-cover of Khartoum using fuzzy classification. *Emir. J. Eng. Res.* **2008**, *13*, 43.
52. Zhang, J.; Foody, G.M. A fuzzy classification of sub-urban land cover from remotely sensed imagery. *Int. J. Remote Sens.* **1998**, *19*, 2721–2738. [CrossRef]
53. Zhou, W.; Troy, A.; Grove, M. Object-based Land Cover Classification and Change Analysis in the Baltimore Metropolitan Area Using Multitemporal High Resolution Remote Sensing Data. *Sensors* **2008**, *8*, 1613–1636. [CrossRef]
54. Yan, G.; Mas, J.F.; Maathuis BH, P.; Xiangmin, Z.; Van Dijk, P.M. Comparison of pixel-based and object-oriented image classification approaches—A case study in a coal fire area, Wuda, Inner Mongolia, China. *Int. J. Remote Sens.* **2006**, *27*, 4039–4055. [CrossRef]
55. Fleiss, J.L.; Levin, B.; Paik, M.C. *Statistical Methods for Rates and Proportions*; John Wiley & Sons, Inc.: Hoboken, NJ, USA, 2003.
56. Foody, G.M. Harshness in image classification accuracy assessment. *Int. J. Remote Sens.* **2008**, *29*, 3137–3158. [CrossRef]
57. Doxani, G.; Siachalou, S.; Tsakiri-Strati, M. An object-oriented approach to urban land cover change detection. *Int. Arch. Photogramm. Remote Sens. Spat. Inf. Sci.* **2008**, *37*, 1655–1660.
58. Congalton, R.G.; Green, K. *Assessing the Accuracy of Remotely Sensed Data: Principles and Practices*; CRC Press: Boca Raton, FL, USA, 2019.
59. Kumar, K.S.; Bhaskar, P.U.; Kumari, K.P. A novel approach for prediction of future environmental impacts of urban growth. *Int. J. Civ. Eng. Technol.* **2018**, *9*, 1208–1219.
60. Mas, J.-F.; Kolb, M.; Paegelow, M.; Olmedo, M.T.C.; Houet, T. Inductive pattern-based land use/cover change models: A comparison of four software packages. *Environ. Model. Softw.* **2014**, *51*, 94–111. [CrossRef]
61. Naghibi, F.; Delavar, M.R.; Pijanowski, B. Urban Growth Modeling Using Cellular Automata With Multitemporal Remote Sensing Images Calibrated By The Artificial Bee Colony Optimization Algorithm. *Sensors* **2016**, *16*, 2122. [CrossRef]
62. Nguyen, T.A.; Le, P.M.T.; Pham, T.M.; Hoang, H.T.T.; Nguyen, M.Q.; Ta, H.Q.; Phung, H.T.M.; Le, H.T.T.; Hens, L. Toward a sustainable city of tomorrow: A hybrid Markov–Cellular Automata modeling for urban landscape evolution in the Hanoi city (Vietnam) during 1990–2030. *Environ. Dev. Sustain.* **2019**, *21*, 429–446. [CrossRef]
63. Pérez-Vega, A.; Mas, J.F.; Ligmann-Zielinska, A. Comparing two approaches to land use/cover change modeling and their implications for the assessment of biodiversity loss in a deciduous tropical forest. *Environ. Model. Softw.* **2012**, *29*, 11–23.
64. Ramachandra, T.V.; Bharath, H.A.; Vinay, S.; Joshi, N.V.; Kumar, U.; Rao, K.V. Modelling urban revolution in greater bangalore, India. In Proceedings of the 30th Annual In-House Symposium on Space Science and Technology, ISRO-IISc Space Technology Cell, Indian Institute of Science, Bangalore, India, 7–8 November 2013; pp. 7–8.
65. Mishra, V.N.; Rai, P.K.; Prasad, R.; Punia, M.; Nistor, M.M. Prediction of spatio-temporal land use/land cover dynamics in rapidly developing Varanasi district of Uttar Pradesh, India, using geospatial approach: A comparison of hybrid models. *Appl. Geomatics* **2018**, *10*, 257–276. [CrossRef]

66. Roy, H.G.; Fox, D.M.; Emsellem, K. Predicting Land Cover Change in a Mediterranean Catchment at Different Time Scales. In *International Conference on Computational Science and Its Applications*; Springer: Cham, Switzerland, 2014; pp. 315–330. [CrossRef]
67. Dzieszko, P. Land-cover modelling using corine land cover data and multi-layer perceptron. *Quaest. Geogr.* **2014**, *33*, 5–22. [CrossRef]
68. Gibson, L.; Münch, Z.; Palmer, A.; Mantel, S. Future land cover change scenarios in South African grasslands—Implications of altered biophysical drivers on land management. *Heliyon* **2018**, *4*, e00693. [CrossRef]
69. Ansari, A.; Golabi, M.H. Prediction of spatial land use changes based on LCM in a GIS environment for Desert Wetlands—A case study: Meighan Wetland, Iran. *Int. Soil Water Conserv. Res.* **2018**, *7*, 64–70. [CrossRef]
70. Pinto, N.; Cox, D.; Dicarlo, J.J. Why is Real-World Visual Object Recognition Hard? *PLoS Comput. Biol.* **2008**, *4*, e27. [CrossRef]
71. Gibbs, H.K.; Ruesch, A.S.; Achard, F.; Clayton, M.K.; Holmgren, P.; Ramankutty, N.; Foley, J.A. Tropical forests were the primary sources of new agricultural land in the 1980s and 1990s. *Proc. Natl. Acad. Sci. USA* **2010**, *107*, 16732–16737. [CrossRef]
72. Li, S.H.; Jin, B.X.; Wei, X.Y.; Jiang, Y.Y.; Wang, J.L. Using ca-markov model to model the spatiotemporal change of land use/cover in fuxian lake for decision support. *ISPRS Ann. Photogramm. Remote Sens. Spat. Inf. Sci.* **2015**, *2*, 163. [CrossRef]
73. Wang, S.; Zheng, X.; Zang, X. Accuracy assessments of land use change simulation based on Markov-cellular automata model. *Procedia Environ. Sci.* **2012**, *13*, 1238–1245. [CrossRef]
74. Gebrehiwot, S.G.; Bewket, W.; Gärdenäs, A.I.; Bishop, K. Forest cover change over four decades in the Blue Nile Basin, Ethiopia: Comparison of three watersheds. *Reg. Environ. Chang.* **2014**, *14*, 253–266. [CrossRef]
75. Gashaw, T.; Bantider, A.; Mahari, A. Evaluations of Land Use/Land Cover Changes and Land Degradation in Dera District, Ethiopia: GIS and Remote Sensing Based Analysis. *Int. J. Sci. Res. Environ. Sci.* **2014**, *2*, 199–208. [CrossRef]
76. Wubie, M.A.; Assen, M.; Nicolau, M.D. Patterns, causes and consequences of land use/cover dynamics in the Gumara watershed of lake Tana basin, Northwestern Ethiopia. *Environ. Syst. Res.* **2016**, *5*, 1. [CrossRef]
77. Tarasovičová, Z.; Saksa, M.; Blažík, T.; Falťan, V. Changes in Agricultural Land Use in the Context of Ongoing Transformational Processes in Slovakia. *Agriculture/Pol'nohospodárstvo* **2013**, *59*, 49–64. [CrossRef]
78. Gebrelibanos, T.; Assen, M. Land use/land cover dynamics and their driving forces in the Hirmi watershed and its adjacent agro-ecosystem, highlands of Northern Ethiopia. *J. Land Use Sci.* **2013**, *10*, 81–94. [CrossRef]
79. Nega, E.; Heluf, G.; Degefe, T. Analysis of land use/land cover changes in western Ethiopian mixed crop-livestock systems: The case of Senbat watershed. *J. Biodivers. Environ. Sci. (JBES)* **2012**, *2*, 8–17.
80. Nyssen, J.; Munro, N.; Haile, M.; Poesen, J.; Descheemaeker, K.; Haregeweyn, N.; Moeyersons, J.; Govers, G.; Deckers, J. Understanding the environmental changes in Tigray: A photographic record over 30 years. *Tigray Livelihood Pap.* **2007**, *3*, 82.
81. Pender, J.; Gebremedhin, B.; Benin, S.; Ehui, S. Strategies for Sustainable Agricultural Development in the Ethiopian Highlands. *Am. J. Agric. Econ.* **2001**, *83*, 1231–1240. [CrossRef]
82. Leta, M.K.; Demissie, T.A.; Tränckner, J. Modeling and Prediction of Land Use Land Cover Change Dynamics Based on Land Change Modeler (LCM) in Nashe Watershed, Upper Blue Nile Basin, Ethiopia. *Sustainability* **2021**, *13*, 3740. [CrossRef]
83. Aburas, M.M.; Abdullah, S.H.; Ramli, M.F.; Ash'Aari, Z.H.; Ahamad, M.S.S. Simulating and monitoring future land-use trends using CA-Markov and LCM models. *IOP Conf. Ser. Earth Environ. Sci.* **2018**, *169*, 012050. [CrossRef]
84. Brown, D.G.; Walker, R.; Manson, S.; Seto, K. Modeling Land Use and Land Cover Change. In *Land Change Science: Observing, Monitoring and Understanding Trajectories of Change on the Earth's Surface*; Springer: Dordrecht, The Netherlands, 2004; pp. 395–409. ISBN 978-1-4020-2562-4.
85. Ahmed, B.; Ahmed, R. Modeling Urban Land Cover Growth Dynamics Using Multi-Temporal Satellite Images: A Case Study of Dhaka, Bangladesh. *ISPRS Int. J. Geo-Inf.* **2012**, *1*, 3–31. [CrossRef]
86. Al-Sharif, A.A.A.; Pradhan, B. Monitoring and predicting land use change in Tripoli Metropolitan City using an integrated Markov chain and cellular automata models in GIS. *Arab. J. Geosci.* **2013**, *7*, 4291–4301. [CrossRef]
87. Goparaju, L.; Prasad, P.R.; Ahmad, F. Geospatial technology perspectives for mining vis-a-vis sustainable forest ecosystems. *Present Environ. Sustain. Dev.* **2017**, *11*, 219–238. [CrossRef]